Fatigue Life, Fractographic and Thermographic Analysis of Steel X2CrNiMo17-12-2 for Proportional and Non-Proportional Loads

D. Skibicki[1], J. Sempruch[2], A. Lipski[3] and Ł. Pejkowski[4]

[1] University of Technology and Life Sciences, Faculty of Mechanical Engineering, Al. Kaliskiego 7, 85-789 Bydgoszcz, Poland, dariusz.skibicki@utp.edu.pl
[2] semjan@utp.edu.pl
[3] adam.lipski@utp.edu.pl
[4] lukasz.pejowski@utp.edu.pl

ABSTRACT. *The article includes the analysis of the results of fatigue testing of austenitic steel X2CrNiMo17-12-2 in as-delivered condition and after annealing. The steel selected was identified in terms of monotonic properties, the chemical composition and the microstructure. The samples for testing were exposed to fully reversed loads, sinusoidally variable: tension-compression, torsion, proportional load produced by tension-compression and torsion at various ratios of amplitudes as well as non-proportional complex load produced by tension-compression and torsion of various ratios of amplitudes and the phase shift angle φ=90. The paper covers a detailed analysis of the correlation between: fatigue life values and loading, fractography of fatigue fractures and loading, strains, stresses parameters and thermographic analysis results.*

INTRODUCTION

Non-proportionality is an important feature of fatigue loading. In case of materials characterized by low stacking fault energy, the non-proportionality reduces fatigue life by several to several dozen times. Therefore it is very important to learn the material behaviour at such loading conditions.

The paper includes comparison of the results of fatigue testing of X2CrNiMo17-12-2 steel under uniaxial loading, multi-axial proportional loading and multi-axial non-proportional loading. This steel grade was selected for tests as it is characterized by high sensitivity to non-proportional loading resulting from its stacking fault energy amounting to 25 MJ/m^2. The steel was tested in as-delivered condition and after annealing.

The analysis included, first of all, the fatigue lives and fractures of specimens. The analysis was extended by comparative analysis of the results of thermographic measurements of specimen surfaces performed during fatigue tests, including plastic strain values and plastic strain energy. Analyses of that kind are rare for multi-axial load [1, 2], but they can bring interesting information on material effort state.

TEST DESCRIPTION

Testing program

The following types of oscillatory, sinusoidal loading were used for the discussed tests: tension-compression, torsion, combined proportional load including tension-compression and torsion with the amplitude ratio of $\lambda = 0.5$ as well as combined non-proportional loading including tension-compression and torsion with the amplitude ratio of $\lambda = 0.5$ or 0.826 and the phase angle of $\varphi = 90°$. S-N and N_{exp}-N_{cal} diagrams were generated for loads defined as above and the fatigue fractures were examined.

Tests of plastic strain, plastic strain energy and thermographic tests were performed for all types of loading, but only for one common equivalent stress value amounting to $\sigma_{eq} = 330$ MPa. Nominal amplitudes of loading are shown in Table 1.

Table 1. Main loading parameters assumed in the research for the equivalent stress level of $\sigma_{eq} = 330$ MPa

load type		σ_a, MPa	τ_a, MPa	φ, °	λ
1	tension-compression	330.0	0.0	0	-
2	torsion	0.0	273.1	0	-
3	proportional	282.5	141.2	0	0.5
4	non-proportional	330.0	165.0	90	0.5
5	non-proportional	330.0	272.6	90	0.8

Test station

The research was carried out using biaxial testing machine Instron 8874 with the load range ±25 kN for tension-compression and ±100 Nm for torsion (Fig. 1a).

a) b)

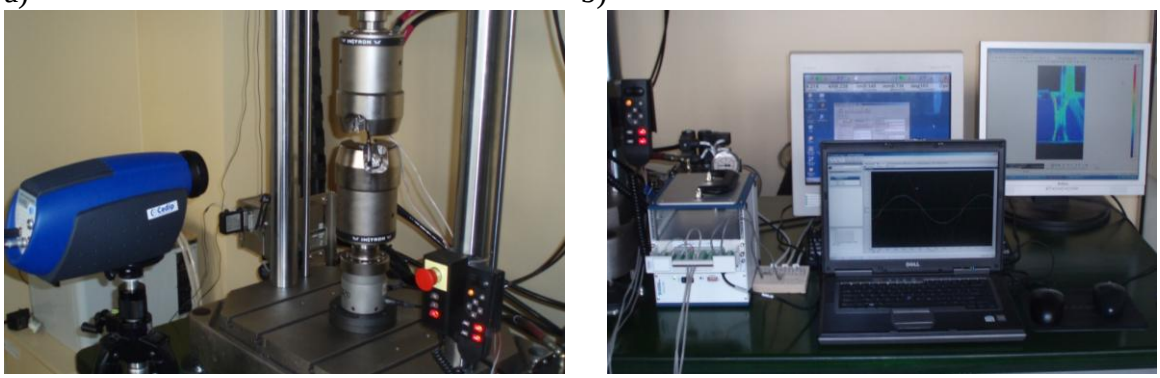

Figure 1. CEDIP Silver 420M thermographic camera aiming at the sample installed in the handle of the testing machine Instron 8874 (a) and the extensometric bridge and the computer controlling Instron 8874 machine as well as computers retrieving data from the extensometric bridge and the thermographic camera (b)

The tensometric research was performed using 8-channel, versatile tensometric bridge NI SCXI-1520 manufactured by National Instruments – and NI SCXI-1600 USB module for data acquisition (Fig. 1b). 1-RY85-0.6/120#-3-3m strain rosettes manufactured by HBM, with measuring base of 0.6 mm and quick-drying adhesive 1-Z70 were also used.

The surface temperature distribution of the samples was additionally recorded with the frequency of 50 Hz using thermographic camera CEDIP Silver 420M (resolution: 320×256 pixels, spectral range: 3.6÷5.0 μm, sensitivity: below 20 mK (available: 8 mK), recording frequency at maximum: up to 140 Hz (up to 25 kHz at the resolution of 64x8 pixels), programmable integration time in the range from 10 μs to 10 ms). Camera images were transmitted via USB 2.0 interface to PC with appropriate software, where they were digitally recorded directly on HDD.

Test specimen

The results of the chemical composition test of X2CrNiMo17-12-2 steel were presented in Table 2.

Full annealing was performed in the electric vacuum furnace with protective atmosphere of argon. Specimens were heated up to the temperature of 1050°C, then held at that temperature for 2 hours and cooled down inside the furnace to the temperature of 620°C. The specimens were then taken out of the furnace and cooled in the open air. The grain size for the specimens in as-delivered condition was g = 8, while for fully annealed specimens amounted to g = 5.

Basic mechanical properties of the tested steel were also determined. For non-annealed material researchers obtained the following results: UTS = 416 MPa, TYS = 210 MPa, HV10 = 234 while for annealed steel UTS = 589 MPa, TYS = 240 MPa, HV10 = 153.

Test samples (specimens) were prepared in accordance with the standard ASTM E2207-02 (Fig. 2).

Table 2. Chemical composition of X2CrNiMo17-12-2 steel

Fe	C	Si	Mn	P	S	Cr	Mo	Ni
63,9	0,028	0,25	1,48	0,033	<0,005	18,03	2,22	12,3

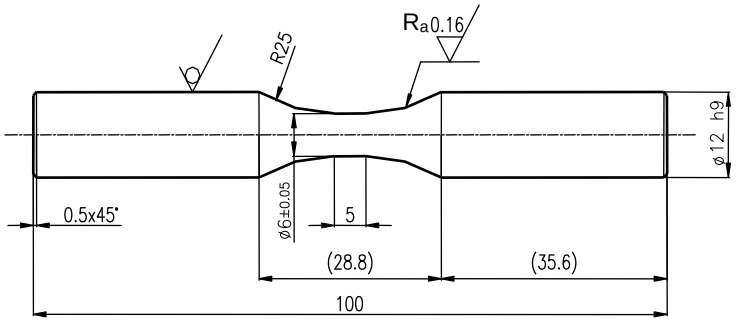

Figure 2. Fatigue test sample

TEST RESULTS

Fatigue life

S-N fatigue life curves were generated as part of the testing, for tension-compression and for torsion (see Fig. 3 (a) and (b)). The obtained results were approximated using linear functions in bilogarythmic scale. In both cases, the fatigue curves of torsion are located under fatigue curves of tension-compression. While for the material in as-delivered condition, both curves are roughly parallel. Whereas for annealed material, the torsion curve in more inclined as compared to the tension curve.

Using Zenner criterion [3], authors proposed amplitude values for complex proportional load – i.e. for tension-compression with torsion of two different amplitude ratios $\tau_a/\sigma_a = 0.5$ and 0.826. Achieved fatigue life values for uniaxial and proportional loading were reflected in the N-N curve, i.e. in Fig. 3(c) for steel in as-delivered condition and in Fig. 3(d) for annealed material. In the first case, almost all results were within the scatter range of width 2, while in the latter case, within 3.

Next, fatigue tests under non-proportional loading were performed. The tests were executed for tension and torsion with nominal amplitude ratio of $\tau_a/\sigma_a = 0.5$ i 0.826 and for phase angle of $\varphi = 90°$. Fatigue life values obtained under non-proportional loading conditions are much lower as compared to those obtained under uniaxial and complex proportional loading and the bigger the non-proportionality the smaller the fatigue life – for loading of $\tau_a/\sigma_a = 0.826$ fatigue lives are smaller than for amplitude ratio of 0.5, Fig. 3 (e). Fatigue lives for $\tau_a/\sigma_a = 0.5$ are within the scatter range of 3, while for $\tau_a/\sigma_a = 0.5$ they are beyond that range Fig. 3 (f).

Fatigue fractures

In case of tension-compression, the fatigue fracture is perpendicular to the loading direction (Fig. 4). Fractures started from a single source located on the specimen surface.

In case of torsion, at high stresses, the macro-fracture direction reflected the direction of maximum tangent stress. Reduction of the stress amplitude resulted in change of the macro-fracture direction by 45°, which indicates that it was perpendicular to the directions of the main stress. The characteristic feature of the fracture was its development in both planes. After further reduction of the tangent stress amplitude, the fracture was still perpendicular to the direction of the main stress but it occurred in only one plane of that stress.

For proportional load with amplitude ratios of $\tau_a/\sigma_a = 0.5$ fractures were perpendicular to the specimen centre line. While for load patterns with greater share of tangent load, i.e. for amplitude ratios of $\tau_a/\sigma_a = 826$ fractures were rotated by about 20° with relation to the specimen centre line. This direction is perpendicular to the direction of the main stresses. In both cases, the fatigue fractures were similar to those of tension-compression fractures.

Non-proportional loading caused more irregular fracture trace on the specimen surface. For loading with amplitude ratios of $\tau_a/\sigma_a = 0.5$ fractures were perpendicular to the direction of main stresses, while for loading with amplitude ratios of $\tau_a/\sigma_a = 0.826$, fractures were perpendicular to the specimen centre line.

(a) tension-compression and torsion for material in as-delivered condition

(b) tension-compression and torsion for annealed material

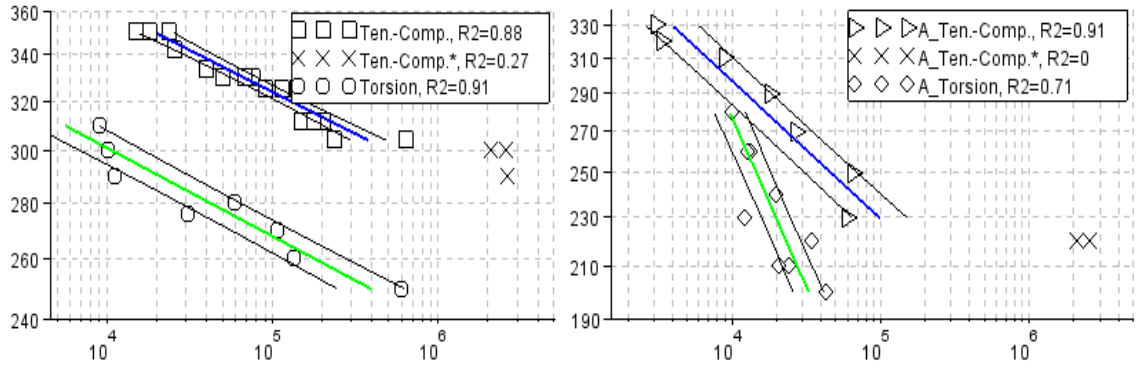

(c) uniaxial and proportional loading for material in as-delivered condition

(d) uniaxial and proportional loading for annealed material

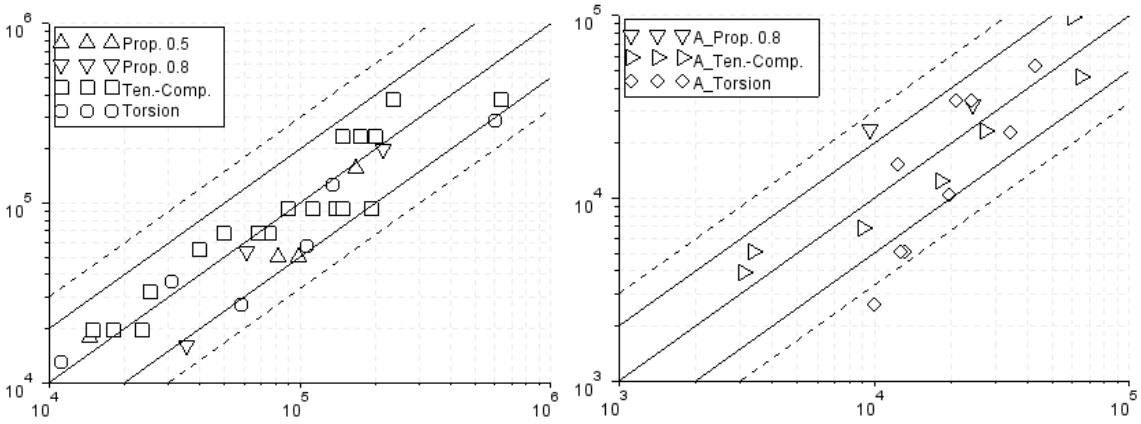

(e) proportional and non-proportional loading

(f) proportional and non-proportional loading

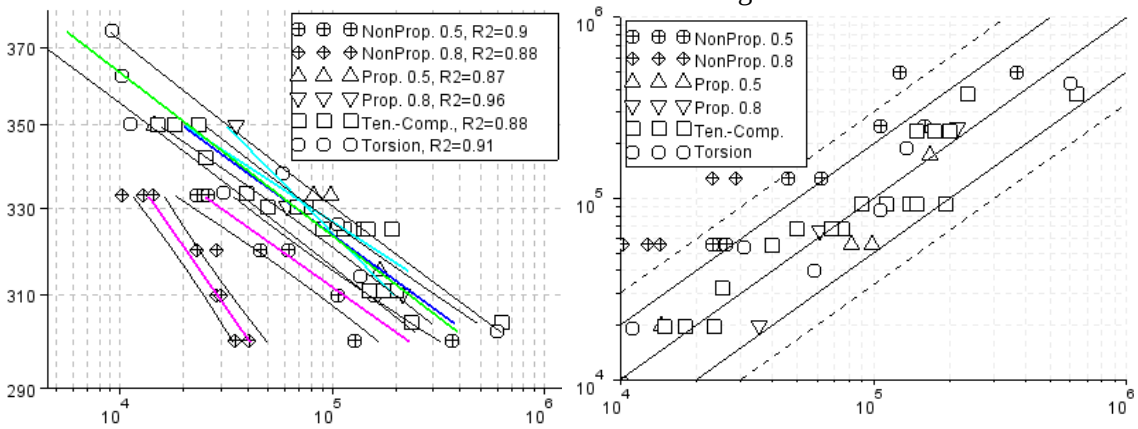

Figure 3. The steel fatigue life results under proportional and non-proportional loading for steel in as-delivered and annealed condition

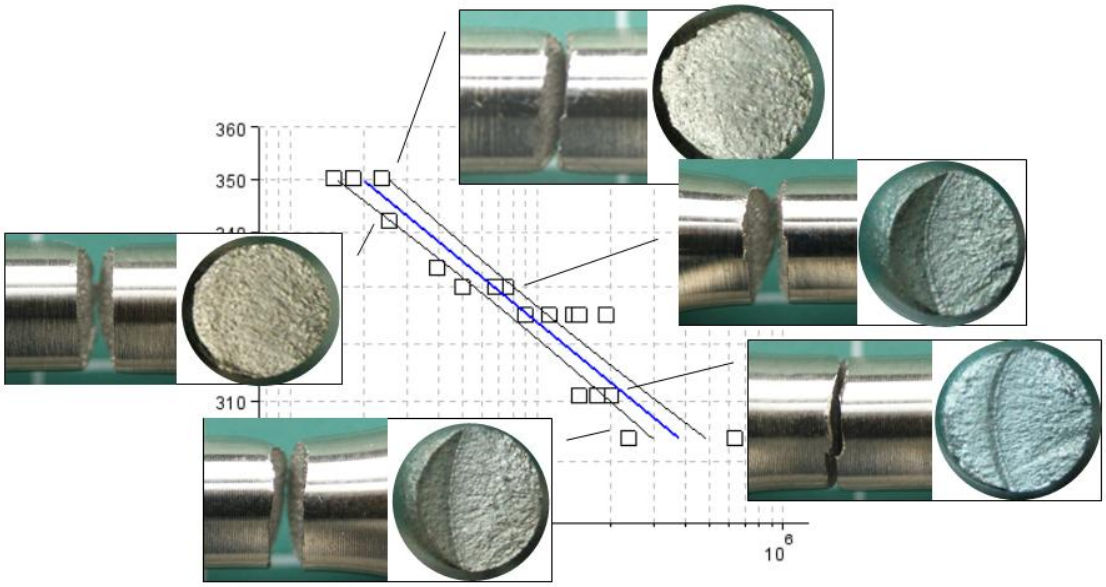

Figure 4. Fractography of specimens for tension-compression

Analysis of strain and thermographic parameters

Cyclic changes of surface temperature were recorded during fatigue tests. Authors analysed curves of continuous temperature changes and, as a result, single cycles characterized by average temperature value T_m and amplitude T_a were distinguished.

Fig. 5 (a) shows the curve of average temperature T_m changes for individual types of loading. Several characteristic stages may be distinguished in those curves:

I – fast increase of the average temperature related to initial loading phase,

II – stable increase of the average temperature of the specimen,

III – fast increase of the average temperature related to final loading phase,

IV – sudden, several-stage increase of temperature related to specimen failure.

The specimen surface temperature changed from the loading start to the specimen failure by 2 to 3°C.

Fig. 6 shows the amplitude of the specimen surface temperature changes T_a recorded for individual types of load during period corresponding to 50% of their life. The value of the temperature amplitude for individual types of loading was virtually constant over the entire period of specimen life. The highest amplitude was obtained for non-proportional loading $\tau_a/\sigma_a = 0.5$ – $T_a = 0.32$°C and for tension-compression – $T_a = 0.31$°C. While for the non-proportional loading $\tau_a/\sigma_a = 0.826$, the amplitude amounted to $T_a = 0.27$°C and for proportional loading – $T_a = 0.24$°C. The lowest amplitude was obtained for torsion – $T_a = 0.04$°C.

For comparison with the temperature changes, Fig. 5 (b) shows changes of plastic strain energy W_{pl}, while Fig. 5 (c) shows changes of plastic strain ε_{pl}.

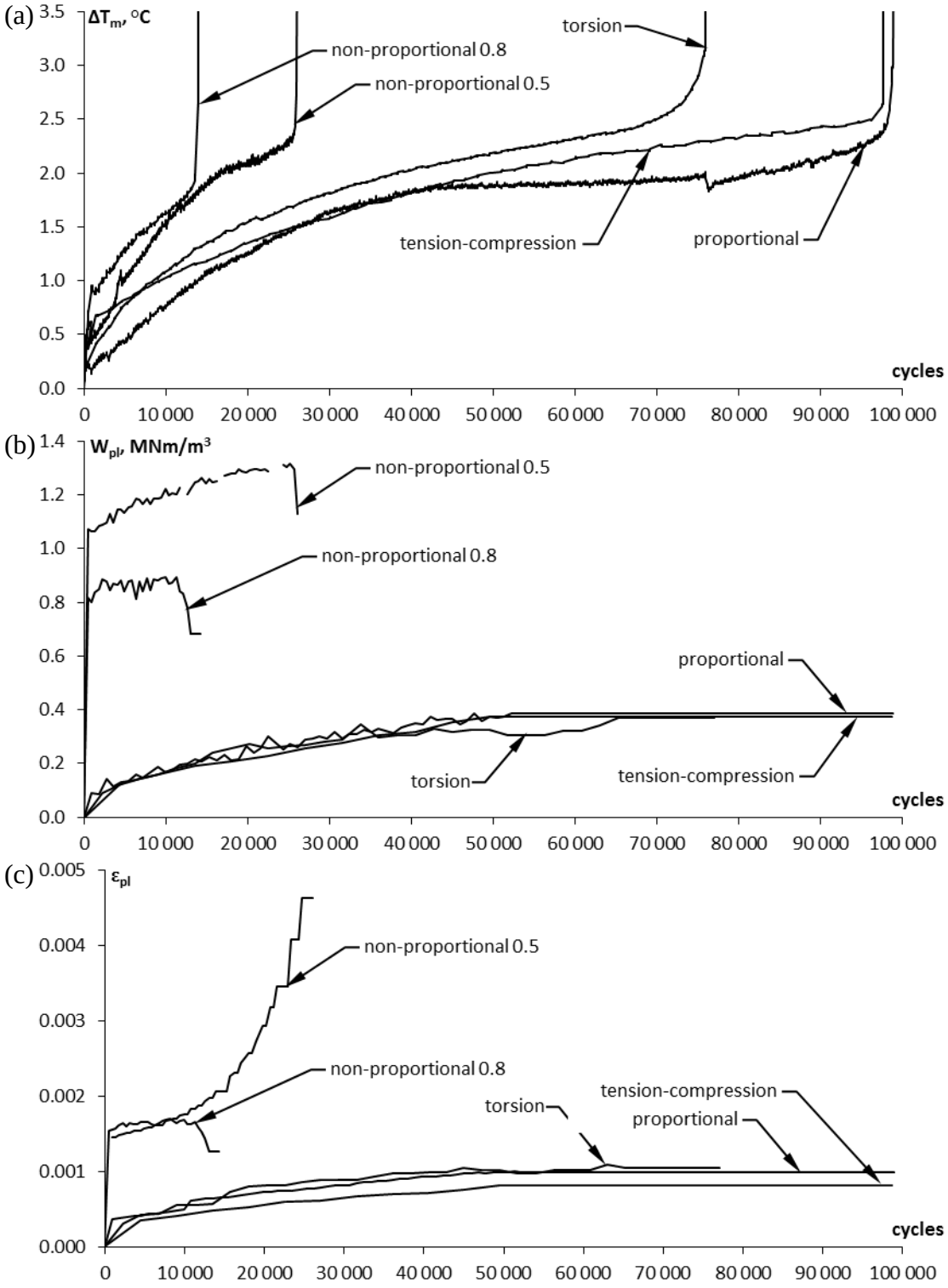

Figure 5. Changes of average specimen surface temperature ΔT_m recorded for individual loading types (a), changes of plastic strain energy W_{pl} (b) and changes of plastic strain ε_{pl} (c)

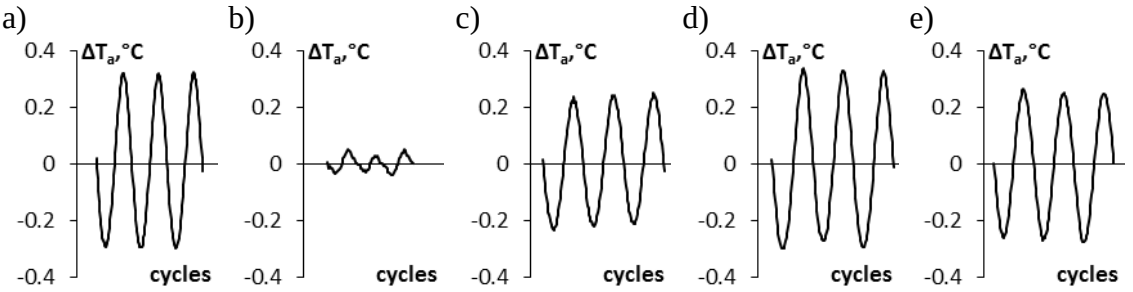

Figure 6. Amplitude changes of specimens surface temperature T_a recorded for individual types of loading during period corresponding to 50% of their life: a) tension-compression, b) torsion, c) proportional, d) non-proportional 0.5, e) non-proportional 0.8

CONCLUSIONS

1. Annealing of X2CrNiMo17-12-2 steel resulted in change of the inclination angle of the fatigue life curve related to torsion as compared to tension curve and caused increase of scattering of the results.
2. X2CrNiMo17-12-2 steel is sensitive to non-proportional loading.
3. The Zenner criterion describes fatigue life under uniaxial and proportional loading, but it is not suitable for description of non-proportional load.
4. Form of fractures for uniaxial and proportional loading corresponds to descriptions provided in the professional literature. Fracture traces for non-proportional loading are irregular and it is hard to correlate their directions with stresses.
5. The curve of the average specimen temperature changes is significantly different in case of non-proportional loading as compared to that of proportional loading and it is always similar to plastic strain energy curve and plastic strain curve.
6. Temperature change amplitude for torsion is several times lower than for other loading types, despite the fact that the equivalent strain value was the same for those loading types.

ACKNOWLEDGEMENTS

The project has been financed from the National Centre for Science.

REFERENCES

1. Poncelet M. et al. (2010): *Probabilistic multiscale models and measurements of self-heating under multiaxial high cycle fatigue*. Journal of Mechanics and Physics of Solids **58** (2010) 578–593.
2. Doudard C. et al. (2007): *Determination of an HCF criterion by thermal measurements under biaxial cyclic loading.* International Journal of Fatigue **29** (2007) 748–757.
3. Zenner H. et al. (2000): *On the fatigue limit of ductile metals under complex multiaxial loading*, International Journal of Fatigue **22** 137-145.